JOURNAL OF MATERIALS SCIENCE 39 (2004) 1721–1725

Microcrack nucleation and its effect on the plastic deformation of FL γ-TiAl alloy

R. T. ZHENG
Key Laboratory of Radiation Beam Technology and Materials Modification of Ministry of Education, Institute of Low Energy Nuclear Physics, Beijing Normal University, Beijing 100875, People's Republic of China
E-mail: ruiting_zheng@yahoo.com.cn

Y. G. ZHANG, C. Q. CHEN
Material Science and Engineering Department, Beijing University of Aeronautics and Astronauts, Beijing 100083, People's Republic of China

Microcracks and their effect on the plastic deformation of γ-TiAl alloy with fully lamellar microstructure (FL) at relatively low strain rate (1×10^{-5}/s) has been investigated. It is found that a large number of microcracks nucleate within the grains. The microcrack density increases with the increase of grain size. Most of the microcracks nucleate at the γ/α_2 interfaces and gather at grains with soft-orientations. Based on the observation and analysis, a model of microcrack nucleation in FL γ-TiAl alloy is built up. The plastic elongation of γ-based TiAl alloys with FL microstructure changes non-monotonously with the increase of grain size, which results from cooperation of micro-deformations and microcracks.

1. Introduction

Titanium-Aluminid alloys based on γ-TiAl have come to be important candidates as aerospace material because of their low density, high high-temperature modulus/strength retention, and good oxidation resistance. But their poor ambient temperature ductility prevents them from wide application. During the last several years, a great deal of work has been done to improve their ductility. Most of the investigations are focused on composition adjustment and microstructure control [1–3].

Microcracks were found to play an important role in the deformation and fracture behavior of the intermetallics. Through tensile experiments on polycrystalline NiAl at 400°C, Schulson and Barker [4] found that irrespective of grain size, fracture occurs in a brittle manner through a combination of intergranular decohesion and transgranular cleavage. They argued that crack nucleation and propagation rather than grain size are of importance for ductility. Chan and Kim [5] proposed that tensile ductility is driven by the nucleation of a stable microcrack whose length is dominated by K_{IC} or J_{IC} under the imposed stress and strain condition. By assuming that the initial microcrack in the alloy has a length equal to the grain or colony size, they have built up a model to interpret the inverse relationship between plastic elongation and initiation toughness K_{IC} in TiAl alloys. Evangelista [6] pointed out that the lamellar interfaces were the preferred sites for crack nucleation in both lamellar and duplex microstructures. It could be attributed to the anisotropic deformability of the lamellar colonies. But Kim [7] has pointed out although inter-lamellar microcracking should depend on the lamellar orientation, the microcrack usually forms in the translamellar direction because of the plastic incompatibility stress between grains.

Though numerous studies have been done on the microcracks in fully lamellar (FL) TiAl alloys [6–10], little is known about the position of microcrack nucleation and the distribution of microcracks. The small size and quick propagation rate of the microcracks make them hard to observe by the ordinary methods in the course of room-temperature uniaxial tensile experiments. To overcome this difficulty, a series of γ-TiAl alloy of FL microstructure with thick lamellar spacing was employed in this investigation, and room-temperature uniaxial tensile experiments were carried out at the strain rate 1×10^{-5}/s. Based on the observation and analysis, a model of microcrack nucleation in FL γ-TiAl alloy was build up.

2. Experimental

The alloy with a nominal composition of Ti-46.5Al-2Cr-1.5Nb-1V (at.%) was prepared using vacuum arc melting technology. The obtained ingot was hot isostatically pressed (HIP'ed) (1260°C/175 MPa/3 h) in argon atmosphere to eliminate casting porosity. Samples were cut from the ingot and prepared for heat treatment by wrapping in Ta foil and sealing in quartz tubes back-filled with argon to 250 mm Hg.

The microstructures were controlled by a special heat treatment method [11–13]. Samples of four different grain sizes with a similar lamellar spacing

TABLE I Heat treatment condition and the macroscopic mechanical properties of FL γ-TiAl alloys

No.	Heat treatment condition	Grain size (μm)	Lamellar spacing (μm)	Fracture strength (MPa)	Plastic elongation (%)
1	1330°C/30 min + controled FC(4°C/min)	1950	0.9	287	1.5
2	1350°C/OQ + 1200°C/3 h/AC + 1320°C/15 min/controled FC(4°C/min)	1140	0.85	339	1.05
3	1350°C/OQ + 1200°C/3 h/AC + 1320°C/10 min/controled FC(4°C/min)	880	0.88	362	0.7
4	1350°C/OQ + 1200°C/3 h/AC + 1320°C/5 min/controled FC(4°C/min)	450	0.85	373	0.83

OQ, oil quenched; AC, air cooled; FC, Fan cooled.

were obtained, as described in Table I. The average grain sizes of the samples in this study were determined using optical microscopy with the line-intercept method. The mean lamellar spacings were measured by transmission electron microscopy (TEM).

Specimens for mechanical test with a gauge of 15 mm and cross section of 5 mm $\times$ 2 mm were cut from the samples by an electric discharge machine, followed by grinding and Electro-polishing to eliminate the surface damage and make observation convenient. Then the specimens were tested at room temperature in air at a nominal strain rate of 1×10^{-5} s^{-1}. At least three specimens were tested for each condition. Average fracture strength and plastic elongation were listed in Table I.

Microstructures and microcracks were observed using NEOPHOT-2 optical microscope (OM). Fracture surfaces were observed by S-5800 scanning electron microscope (SEM). Backscatter electron (BSE) and energy dispersive X-ray (EDX) analysis were performed in a JSM6301F field emission scanning electron microscope.

3. Results

3.1. The microstructures and the mechanical properties

All microstructures in the present study were FL microstructures. The microstructure parameters as well as the heat treatment processes are listed in Table I. The mechanical properties of the alloys are also listed in Table I. It can be seen from the Table I that, at the strain rate of 1×10^{-5} s^{-1}, the fracture strength increased with the decrease of the grain size. Fig. 1 shows the relationship between plastic elongation and grain size for FL TiAl alloys with a similar lamellar spacing. It was found that the plastic elongation varied non-monotonously with the increase of grain size. The plastic elongation first decreased and then increased.

3.2. Observation of the specimen surfaces

Fig. 2a shows the typical specimen surface near the fracture facet. It can be seen from Fig. 2a that there are three main features in the surface: (A) blunt microcracks along lamellae interfaces or at the grain boundaries; (B) interlamellar slip along the lamellar interfaces; and (C) planar cross slip, which exhibited a wavy appearance and intersected with the lamellar interfaces. Microcracks and interlamellar slip were distributed all over the specimen surface, but planar cross slip only appeared near the fracture facet. Fig. 2b and c show the surfaces of the No. 1 and No. 4 specimens, respectively. The average grain size in the No. 1 specimen was the largest among all specimens, while No. 4 specimen was smallest. Different from other prior observations [14, 15] and hypotheses [5], many microcracks were present within some special grains in this investigation. Namely, microcracks gathered within the grains with soft orientations (i.e., the angle between the lamellar direction and the tensile axis is close to 45°), and few

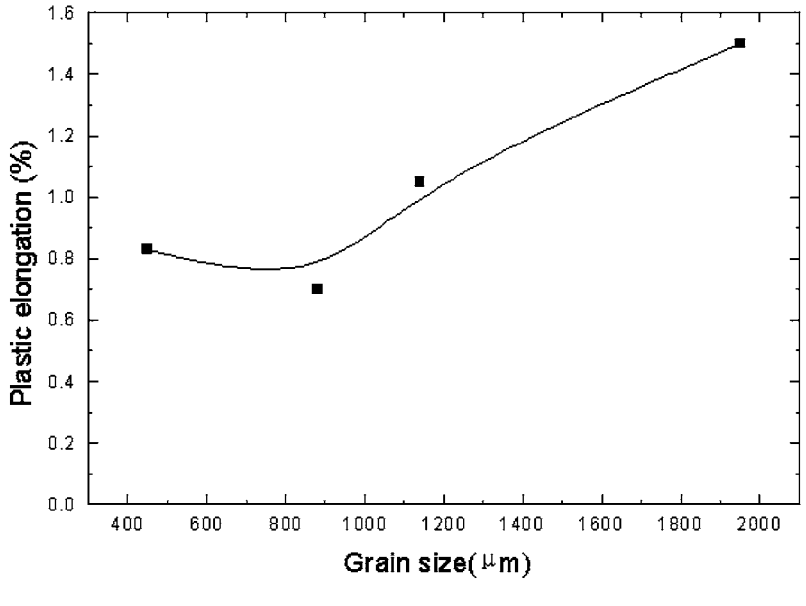

Figure 1 Relationship between plastic elongation and grain size for FL TiAl alloys.

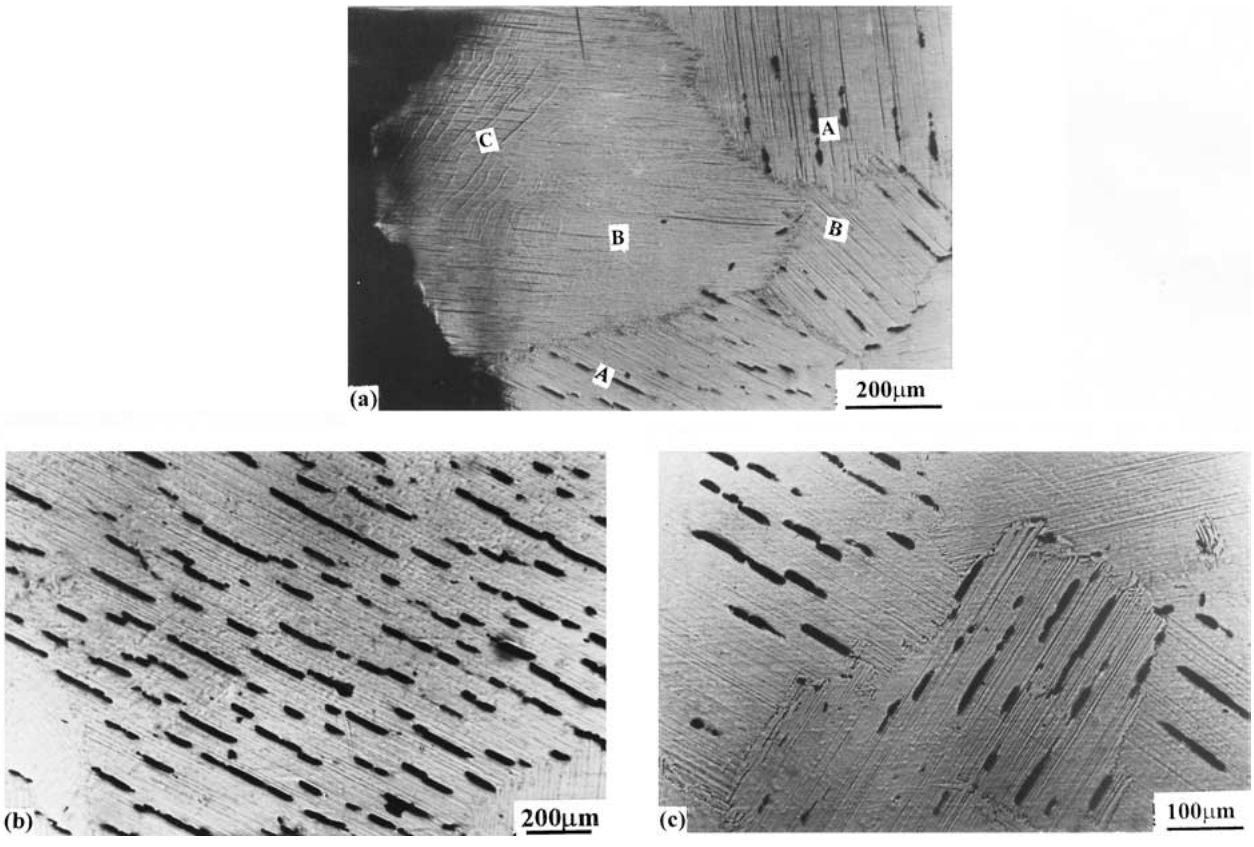

Figure 2 OM photographs of specimen surfaces: (a) Deformation feature near the fracture surface, (b) Surface of specimen with large grain size, and (c) Surface of specimen with small grain size.

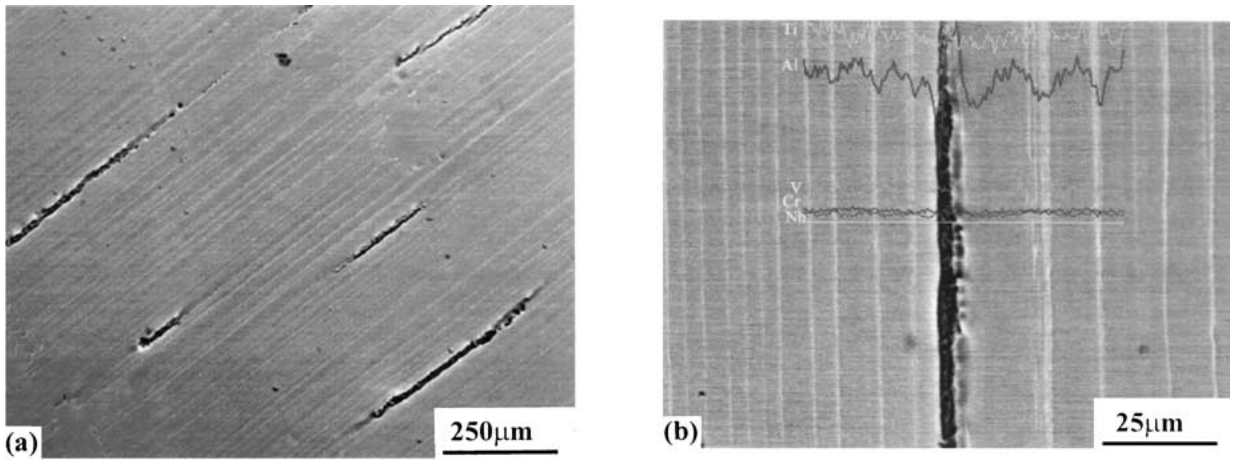

Figure 3 Back scatter electron image of the specimen surface: (a) The BSE images of the fractured specimen surface and (b) Components analysis near a crack.

cracks appeared within the grains with hard orientation (i.e., the angle between the lamellar directions and the tensile axis is close to 0° or 90°). The larger grain size of the specimens, the more microcracks they have. Most of the microcracks formed along the lamellar interfaces, and a few nucleated at the grain boundaries. It is believed that they are related to strain incompatibility between adjacent lamellae.

Backscatter electron (BSE) images and EDX were employed to find out the relationship between the positions of the microcracks and the phase distribution. Fig. 3a shows a BSE image of a typical specimen surface. Light stripes were identified as Ti_3Al (α_2) and dark stripes were identified as TiAl (γ). It could be seen that microcracks generally nucleated along the α_2 plates. In order to confirm this observation, EDX analysis was done along the normal line of a microcrack as illustrated in Fig. 3b. Components distribution shows that the phase on the left side of the microcrack was α_2, which has a low content of Al. While the phase on the right side of the microcrack was γ, which has a high content of Al. The microcrack lies at the position of α_2/γ interface. This is consistent with the observations for PST (polysynthetically twinned) TiAl alloys [16].

3.3. Observation of the fracture surfaces

The typical fracture surfaces of tensile specimen tested at 1×10^{-5} s^{-1} are shown in Fig. 4. Fractographic studies revealed a composite fracture appearance, both

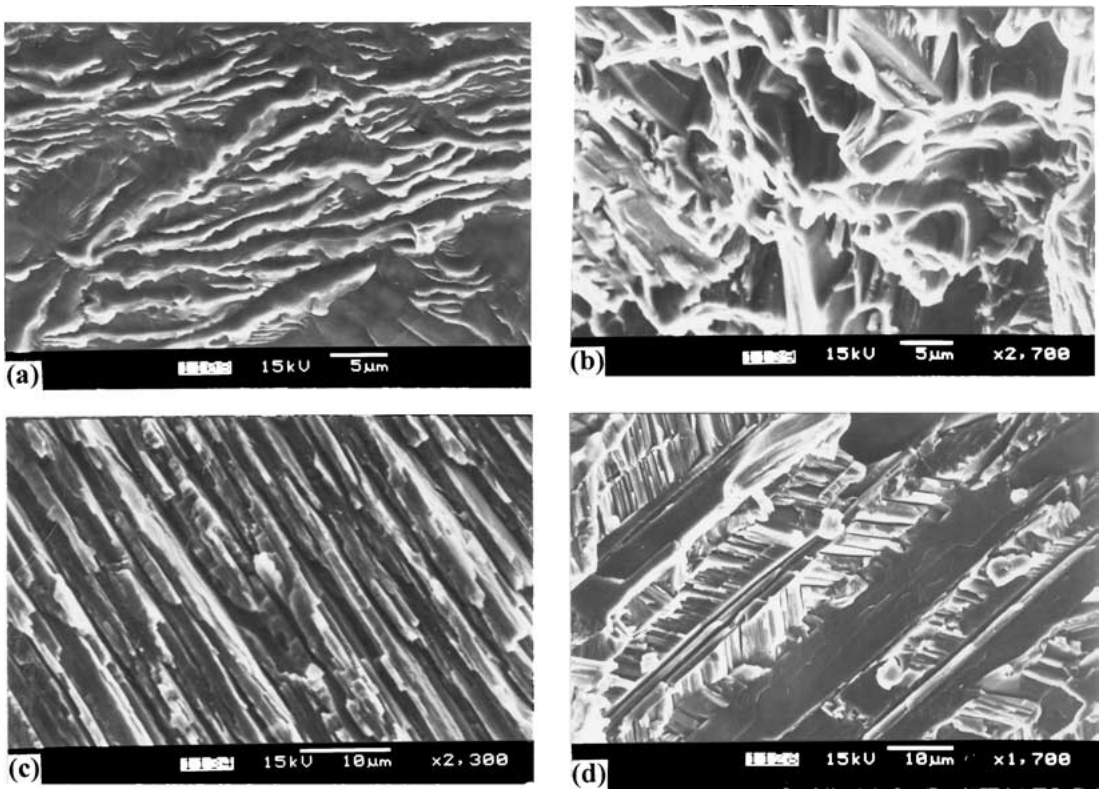

Figure 4 SEM micrographs of typical fracture surfaces: (a) Low energy interface facet, (b) Dimpled fracture surface, (c) Delamination of lamellae, and (d) Decohesion microtwin planes.

translamellar fracture (across the lamellae) and delamination of interfaces resulting in apparent low-enerage facets on the fracture surface were observed. Fracture characteristics similar to those shown in Fig. 4a and c were reported in previous study [17, 18]. The current results differ from their observations in that the low energy interfaces observed in this experiment were full of ridges (Fig. 4a). They were the result of translamellar slip of ordinary dislocations. The dimple fracture surface in Fig. 4b looks unlike what is usually exhibited in tensile experiment at the high temperature [17] (above 800°C). It shows somewhat brittle characteristics. In many instances, translamellar crack propagation was accompanied with concurrent interface delamination (Fig. 4c). Fracture surfaces such as that shown in Fig. 4d have never been reported before. It could be seen that a lot of cleavage facets intersect with the lamellar interface. Since the cleavage facets paralleled to each other in one plate and changed direction in the neighboring plate, they are probably cross-twin planes within γ lamellae as discovered by Huang *et al*. [19].

4. Discussion

4.1. Microcrack nucleation

The slip planes in the γ phase are the {111} planes. Slip of ordinary dislocations $\frac{1}{2}\langle 1\bar{1}0]$ is relatively easy at ambient temperature because of a low critical resolved shear stress. In comparison, the activation of superlattice dislocations in the $\langle 10\bar{1}]$ slip directions is difficult at ambient temperature. Though $\langle 11\bar{2}]\{111\}$ ordered twins generally exist at ambient temperature, it cannot take place of the role of independent slip systems [20]. There are four different easy slip systems in γ, only three of them are independent, which is far less than the five independent slip systems required for arbitrary plastic deformation. The ordered twins in γ plates can provide the other two deformation systems for local plastic deformation. But the γ/α_2 interfaces and the α_2 lamellae themselves can be strong barriers to slip and deformation twinning [21]. Therefore, the γ/α_2 interfaces are the main sites for crack nucleation (Fig. 3b).

Deformation in soft-orientation grains is larger than that in hard-orientation grains in γ-TiAl alloys because a higher critical-resolved stress is required to induce slip in translamellar directions than in interlamellar directions. Ordered twins and translamellar slip appears in largely deformed grains with soft-orientations owing to lack of adequate easy slip systems. They will stop at the γ/α_2 interfaces. Large local stresses induced by dislocations groups cannot be released. Consequently microcracks will be formed in these sites with a manner proposed by Stroh [22, 23]. The schematic diagram of microcrack nucleation is shown in Fig. 5.

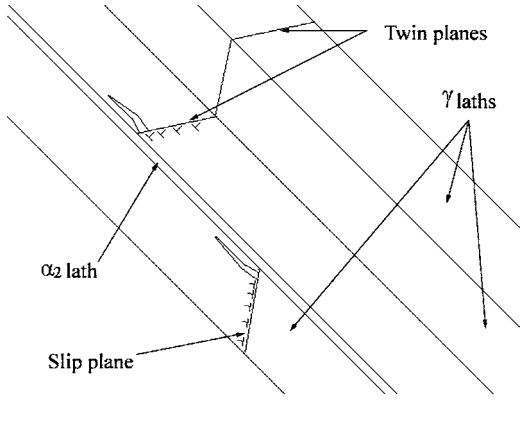

Figure 5 The schematic diagram of the microcrack nucleation in FL TiAl alloy.

Microcracks will nucleate with a type I crack mode under the local tension stress in the γ laths. Then they will propagate along the γ laths with the type II crack mode because of the existence of large shear stress in these directions. Higher energy is stored in lamellar interfaces, so most of microcracks are restricted in one lath before the occurrence of a catastrophic propagation. The size and density of the microcracks depend on the inner stress distribution and the strain rate.

4.2. Ambient temperature ductility

Usually, fine-grained materials have better plasticity because of more grain boundaries and slip planes. It was found that the Hall-Patch equation based on grain size is applicable to TiAl alloys with lamellar microstructures at room temperature and 800°C [24]. But relationship of plastic elongation and grain size in Fig. 1 disobeys such a law during deformation. Ductility does not increase monotonously with the decreasing grain size. The key factor in determining the mechanical properties of most intermetallic compounds is the microstructures. The microstructure of alloys should be taken into consideration to explain this abnormal phenomenon.

At strain rate as low as 1×10^{-5}/s, sufficient deformation occurs in the specimens. Low energy interface facets (Fig. 3a) show the existence of translamellar slip. Dimpled fracture surfaces (Fig. 3b) are the evidence of multiple slip systems. So microcracks propagate slowly and become blunt easily because of a larger crack tip plastic field induced by thick lamellar spacings. It is well known that large grains in an alloy would result in great strain incompatibility, and the slip systems are insufficient to release stress concentration in these alloys. So the microcrack density increases with the increase of grain size. It is clear that the microcrack and the micro-deformation systems are dominant factors of plastic elongation. A competition exists between these two factors. When FL TiAl alloys are deformed in tension at a relatively high strain rate, few microcracks nucleate before the specimen fractures. In this condition, the plastic elongation mainly comes from dislocation slip. With the decrease of grain size, the compatibility between grains improves, and the plastic elongation also increases. In contrast, when FL TiAl alloys are deformed in tension at a relatively low strain rate, a large number of microcracks nucleate and then become blunt. Microcracking turns to be another dominant factor of plastic elongation. With the increase of grain size, the decrease of plastic elongation induced by strain incompatibility is offset by the effect of microcracks. Thus the plastic elongation finally increases.

5. Conclusions

The conclusions in this study are as follows:

1. While the FL TiAl alloys deformed at relative low strain rates (1×10^{-5}/s), a large number of microcracks nucleate within the grains. The microcrack density increases with an increase of grain size.

2. There is regularity for the orientation of microcracks. Most of the microcracks nucleate at the γ/α_2 interfaces and gather at grains with soft-orientations.

3. Microcracks will nucleate with the type I crack mode under the local tension stress in the γ laths. Then they will propagate along the γ laths with the type II crack mode because of the existence of large shear stress in these directions.

4. The plastic elongation of γ-based TiAl alloys with FL microstructure changes non-monotonously with the increase of grain size at the strain rate of 1×10^{-5}/s, which results from cooperation of micro-deformations and microcracks.

Acknowledgement

The authors thank the financial support from China Nature Science Foundation under the contract No. 59895150.

References

1. Y. W. KIM, *JOM* **41**(7) (1994) 24.
2. M. YAMAGUCHI and H. INUI, in "Structural Intermetallics," edited by R. Daralia *et al.* (Warrendale, PA, TMS, 1993) p. 127.
3. S. C. HUANG and J. C. CHESNUTT, in "Intermetallic Compounds and Practice," edited by J. H. Westbrook and R. L. Fleischer, (John Wiley & Son Ltd. 1995) p. 73.
4. E. M. SCHULSON and D. R. BAKER, *Scripta Metall.* **17** (1983) 519.
5. K. S. CHAN and Y. W. KIM, *Metall. Trans.* **23A** (1992) 1663.
6. E. EVANGELISTA, W. J. ZHANG, *et al.*, *Scripta Metall.* **33**(3) (1995) 467.
7. Y. W. KIM, *Mater. Sci. Eng.* A **192/193** (1995) 519.
8. M. H. YOO, J. ZOU and C. L. FU, *ibid.* A **192/193** (1995) 14.
9. HIROHISA SHIOTA, KEIRO TOKAJI and YASUHITO OHTA, *ibid.* A **243** (1998) 169.
10. J. J. M. ARATA, K. S. KUMAR, W. A. CURTIN and A. NEEDLEMAN, *Inter. J. Fract.* **111** (2001) 163.
11. GUOXIN CAO, LIANFENG FU, JIANGUO LIN, *et al.*, *Intermetallics* **8** (2000) 647.
12. JIANCHENG TANG, BAIYUN HUANG, KECHAO ZHOU, WENSHENG LIU, YUEHUI HE and YONG LIU, *Mater. Res. Bull.* **36** (2001) 1737.
13. T. NOVOSELOVA, S. MALINOV and W. SHA, *Intermetallics* **11** (2003) 491.
14. KWAI S. CHAN, BETTINA WITTKOWSKY and MICHAEL PFUFF, *Metall. Trans.* **30A** (1999) 1023.
15. K. S. CHAN and Y. W. KIM, *Acta Metall Mater.* **43**(2) (1995) 439.
16. L. HEATHERLY, JR., E. P. GEORGE, C. T. LIU and M. YAMAGUCHI, *Mater. Sci. Eng.* A **239/240** (1997) 404.
17. K. S. CHAN and Y. W. KIM, *Metall. Trans.* **24A** (1993) 113.
18. J. KUMPFERT, Y. W. KIM and D. M. DIMIDUK, *Mater. Sci. Eng.* A **192/193** (1995) 465.
19. B. Y. HUANG*, Y. H. HE and J. N. WANG, *Intermetallics* **7** (1999) 881.
20. LIANG WEI, LI QIANG and YANG DE ZHUANG, *Acta Metall. Sinica* **33**(3) (1997) 292.
21. T. FUJIWARA, A. NAKAMURA, H. HOSOMI, S. R. NISHITANI, Y. SHIRAI and M. YAMAGUCHI, *Philos. Mag.* A **61** (1990) 591.
22. A. N. STROH, *Proc. Roy. Coc.* **223A** (1954) 404.
23. *Idem.*, *ibid.* **232A** (1955) 232.
24. C. T. LIU and P. J. MAZIASZ, *Intermetallics* **6** (1998) 653.

Received 17 January
and accepted 4 September 2003